Geochemical Perspectives Letters

^{190}Pt-^{186}Os geochronometer reveals open system behaviour of ^{190}Pt-^{4}He isotope system

A. Luguet[1*], G.M. Nowell[2], E. Pushkarev[3], C. Ballhaus[1], R. Wirth[4], A. Schreiber[4], I. Gottman[3]

OPEN ACCESS

doi: 10.7185/geochemlet.1924

Abstract

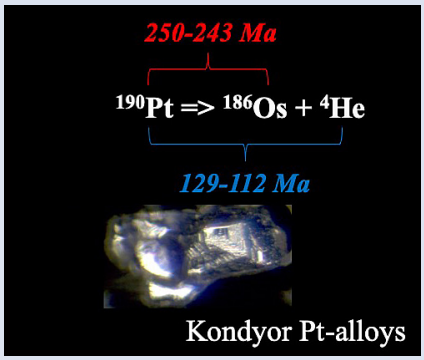

Platinum Group Minerals are typically dated using the ^{187}Re-^{187}Os and ^{190}Pt-^{186}Os isotope systems and more recently using the ^{190}Pt-^{4}He geochronometer. The ^{187}Re-^{187}Os and ^{190}Pt-^{186}Os compositions of Pt-alloys from the Kondyor Zoned Ultramafic Complex (ZUC) analysed here reveal overprinting for both geochronometers except in one alloy exhibiting the most unradiogenic ^{187}Os/^{188}Os and most radiogenic ^{186}Os/^{188}Os signatures. These signatures argue for an Early Triassic mineralisation, when silicate melts/fluids derived from the partial melting of an Archean mantle crystallised to form the Kondyor ZUC while the ^{190}Pt-^{4}He chronometer supports an Early Cretaceous mineralisation. We propose that Kondyor ZUC represents the root of an alkaline picritic volcano that constitutes the remnants of an Early Triassic island arc formed during the subduction of the Mongol-Okhotsk ocean seafloor under the Siberia craton. After the Early Cretaceous collision of Siberia with the Mongolia-North China continent, the exhumation of deep-seated structures - such as the Kondyor ZUC - allowed these massifs to cool down below the closure temperatures of the Pt-He and K-Ar, Rb-Sr isotope systems, explaining their Early to Late Cretaceous ages for the Kondyor ZUC.

Received 19 May 2019 | Accepted 28 August 2019 | Published 22 October 2019

Introduction

Platinum group minerals (PGM, *e.g.*, Os-alloys, Pt-alloys, Pt-arsenides) are critical host phases of the Highly Siderophile Elements (HSE; Os, Ir, Ru, Rh, Pt, Pd, Re) in the Earth's mantle and crust. They are typically dated with the ^{187}Re-^{187}Os and/or ^{190}Pt-^{186}Os isotope systems (*e.g.*, Walker *et al.*, 1997; Meibom and Frei, 2002; Pearson *et al.*, 2007; Coggon *et al.*, 2012).

Recently, the ^{190}Pt-^{4}He isotopic system has emerged as an alternative geochronometer for Pt-rich PGM. The ^{190}Pt-^{4}He and ^{190}Pt-^{186}Os geochronometers are both measuring the alpha decay of ^{190}Pt, with the only difference being that one measures the accumulation of the daughter product ^{186}Os and the other the accumulation of the decay particle ^{4}He. The Pt-He geochronometer was so far used to date the Pt-alloys from the Kondyor Zoned Ultramafic Complex (ZUC), which is located in the Aldan Shield on the South-East margin of the Siberian Craton (Fig. S-1 and Supplementary Information) (Shukolyukov *et al.*, 2012a; Mochalov *et al.*, 2016, 2018). The Early Cretaceous Pt-He isochron ages (112 ± 7 Ma and 129 ± 6 Ma, calculated using a ^{190}Pt half-life of 469 Gyr: Begemann *et al.*, 2001) agree well with the Rb-Sr, Sm-Nd and K-Ar ages obtained on the main lithologies (whole rock and mineral phases) but conflict with the Re-Os T_{RD} model ages obtained on erlichmanite (OsS_2), sperrylite ($PtAs_2$), Os-alloys and Pt-alloys (Cabri *et al.*, 1998; Malitch and Thalhammer, 2002) that vary from Neoproterozoic (658-603 Ma) to future ages, when back calculated to the present-day primitive mantle (PM) ^{187}Os/^{188}Os estimate (Meisel *et al.*, 2001).

The combination of multiple isotope systems for dating single mineral phases offers the opportunity to resolve "open system behaviour" and to assess which isotopic signatures provide geologically meaningful information on the age and origin of minerals. Here we report the coupled ^{190}Pt-^{186}Os and ^{187}Re-^{187}Os signatures obtained by Laser Ablation Multi Collector Inductively Coupled Plasma Mass Spectrometry (LA-MC-ICPMS) (Supplementary Information) on 13 sub-millimetric Pt-alloys separated from a chromitite schlieren (sample 1265; Pushkarev *et al.*, 2015) hosted in the dunitic core of the Kondyor ZUC. Our Pt-alloys are a different subset from those investigated for the ^{190}Pt-^{4}He isotope system. Shukolyukov *et al.* (2012a) and Mochalov *et al.* (2016, 2018) dated (i) Pt-alloys from different lithologies of the Kondyor ZUC, including the chromitite lenses of the dunitic core and

1. Institute of Geosciences, University of Bonn, Germany
2. Earth Sciences Department, University of Durham, UK
3. Russian Academy of Sciences, Institute of Geology and Geochemistry Ural Division, Moscow, Russia
4. Helmholtz Centre Potsdam, GeoForschungs Zentrum, Section 3.5 Surface Geochemistry, Potsdam, Germany
* Corresponding author (email: ambre.luguet@uni-bonn.de)

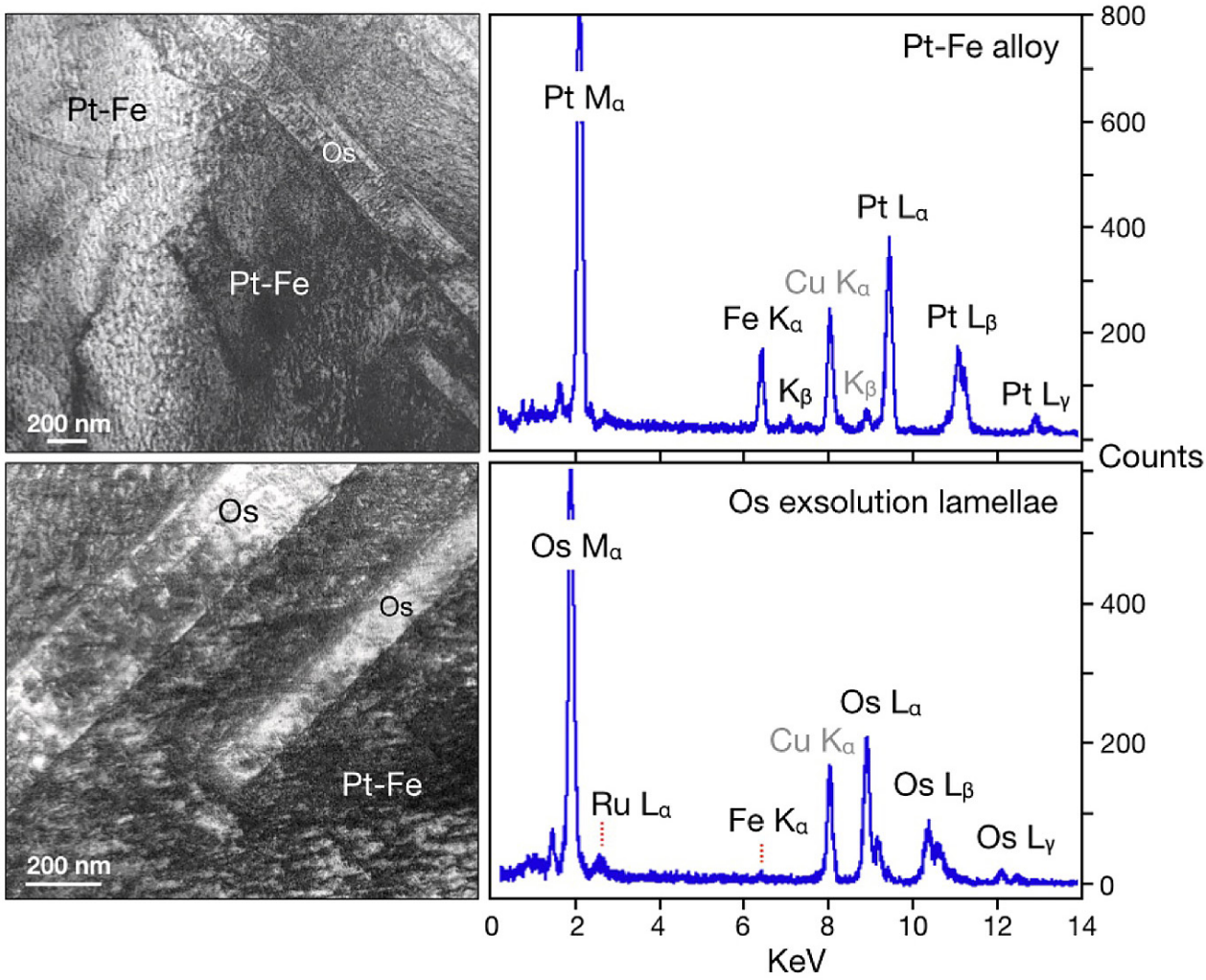

Figure 1 Bright field image and EDS spectra of Kondyor Pt-Fe alloys and their pure Os exsolution lamellae (FIB-TEM image, GFZ, Potsdam, Germany). The Cu peaks on the EDS spectra are due to the Cu grid that carries the FIB section.

(ii) alluvial Pt-Pd PGM. The FIB-TEM investigations on a few of our Pt-alloys revealed a very complex nanoscale exsolution pattern consisting of spinodal exsolutions of Pt-Fe alloys (*e.g.*, Pt_3Fe, PtFe) and pure Os exsolution lamellae (Fig. 1).

Results

The Kondyor Pt-alloys display radiogenic $^{186}Os/^{188}Os$ and unradiogenic $^{187}Os/^{188}Os$ compositions (Fig. 2 a,b). The most radiogenic $^{187}Os/^{188}Os$ signatures (0.1246; alloys L-S2 and E-S2, Table S-2) agree well with those previously obtained on five Kondyor Os-rich alloys (0.1248-0.1252; Malitch and Thalhammer, 2002). Conversely, the least radiogenic $^{187}Os/^{188}Os$ (0.110096 ± 2136; alloy D-S2) is close to the composition of Re-free, least metasomatised peridotite xenoliths of the Tok locality (0.109; estimated for $Al_2O_3 = 0$ wt. % on the $^{187}Os/^{188}Os$ *vs.* Al_2O_3 "aluminochron"; Ionov *et al.*, 2006), which like the Kondyor ZUC is located in the East Aldan Shield (Fig. S-1). Overall, the $^{187}Os/^{188}Os$ compositions are decoupled from the $^{187}Re/^{188}Os$ ratios (Fig. 2a). In contrast, the $^{186}Os/^{188}Os$ compositions define a positive trend with $^{190}Pt/^{188}Os$, which - if considered to represent an isochronous relationship - yields an age of 249.8 ± 12 Ma (Fig. 2b). The $^{187}Os/^{188}Os$ and $^{186}Os/^{188}Os$ signatures are negatively correlated despite the sympathetic variation of both parent/daughter elemental ratios (Fig. 2c).

Robustness of the Re-Os and Pt-Os Isotope Systematics

The decoupling of the $^{187}Os/^{188}Os$ from both $^{187}Re/^{188}Os$ and $^{186}Os/^{188}Os$ signatures demonstrate the open system behaviour of the Re-Os isotope system in the Kondyor Pt-alloys. This is best explained by the overprinting of the Os-poor, least radiogenic $^{187}Os/^{188}Os$ of the Pt-alloy D-S2 by an Os-rich (*ca.* 700 times richer) contaminant with a $^{187}Os/^{188}Os$ of 0.1246 (Fig. 3a), similar to the most radiogenic $^{187}Os/^{188}Os$ of our Kondyor alloys (*e.g.*, points E-S2) and very close to the least radiogenic $^{187}Os/^{188}Os$ compositions previously reported by Malitch and Thalhammer (2002) and Cabri *et al.* (1998) for Kondyor PGM (Fig. 2a). Both the $^{186}Os/^{188}Os$ *vs.* $^{187}Os/^{188}Os$ and $^{186}Os/^{188}Os$ *vs.* 1/Os relationships (Fig. 3b) can be reproduced with such a mixing scenario. Importantly, the negative $^{187}Os/^{188}Os$ *vs.* $^{187}Re/^{188}Os$ and the relationships between the $^{187}Os/^{188}Os$ and the abundance of Os exsolution lamellae (monitored by the ^{188}Os signal) in the Pt-alloys likely suggest that this mixing scenario reflects a gradual overprinting of the mantle source of the Kondyor mineralisation by subduction-related fluids (Supplementary Information).

The Pt-alloy D-S2 is then the least overprinted of our Kondyor subset (Fig. 3a,b). This view is further supported by the closeness of its $^{187}Os/^{188}Os$ and $^{187}Re/^{188}Os$ ratios (0.001196 and 0.00541; Table S-2) to those of the Re-free, least metasomatised Tok peridotite xenoliths (0.109 and 0; Ionov *et al.*, 2006),

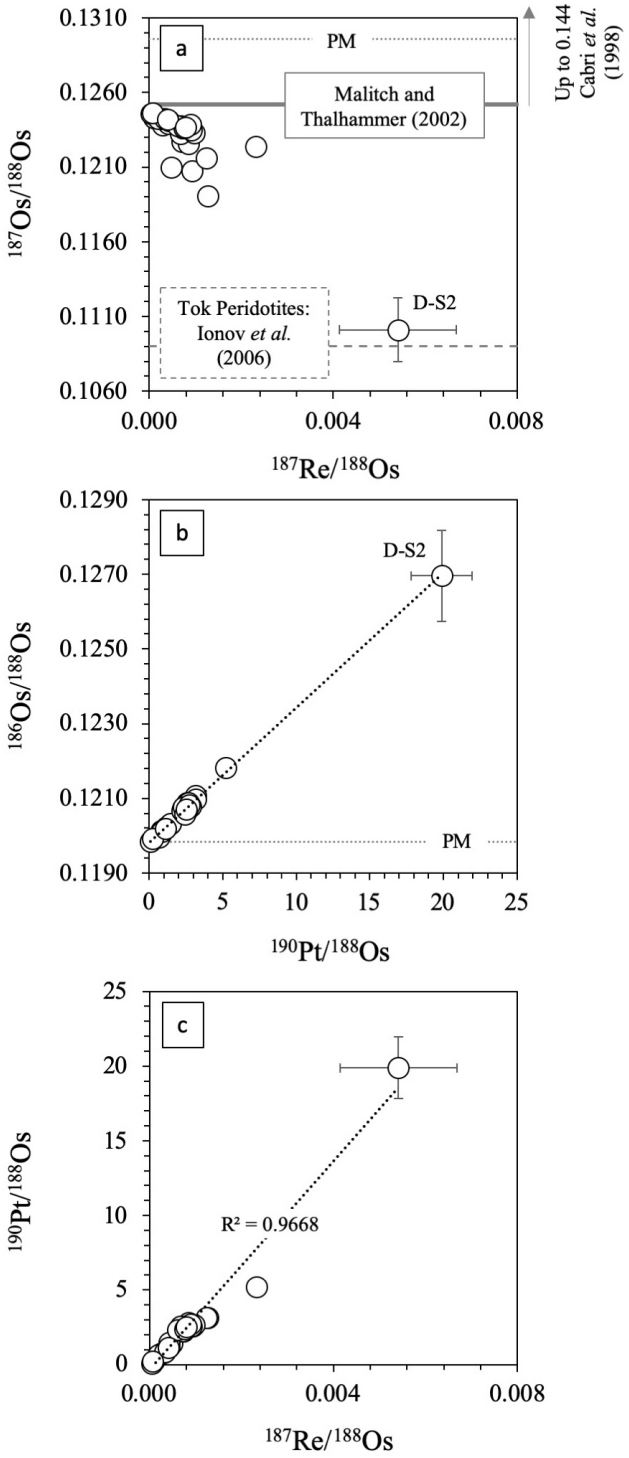

Figure 2 **(a)** Variations of $^{187}Os/^{188}Os$ *vs.* $^{187}Re/^{188}Os$, **(b)** of $^{186}Os/^{188}Os$ *vs.* $^{190}Pt/^{188}Os$ and **(c)** of $^{190}Os/^{188}Os$ *vs.* $^{187}Re/^{188}Os$. The primitive mantle (PM) $^{186}Os/^{188}Os$ and $^{187}Os/^{188}Os$ values are respectively from Day *et al.* (2017) and Meisel *et al.* (2001). If the positive correlation between $^{186}Os/^{188}Os$ *vs.* $^{190}Pt/^{188}Os$ is considered to be an isochronous relationship, it yields an age of 249.8 ± 12 Ma and an intercept of 0.119821 ± 0.000024 (2 sigma) (MSWD = 0.81).

implying that the $^{187}Os/^{188}Os$ composition of alloy D-S2 may still hold geologically meaningful constraints. Its Re-Os T_{RD} model age points at a 2630 Ma old PUM-like mantle source for the Kondyor Pt-mineralisation (the Re-Os T_{MA} model age is 2664 Ma). Occurrence of Archean mantle underlying the Aldan Shield is also supported by the T_{RD} model ages of the Tok peridotites (2770 Ma) and by Pb-Pb isotope systematics of the Mesozoic lamproitic magmatism (~3 Ga; Davies *et al.*, 2006). Considering that the present-day PM has a $^{186}Os/^{188}Os$ of 0.1198388 and a $^{190}Pt/^{186}Os$ of 0.0022 (Day *et al.*, 2017), the 2630 Ma PUM-like mantle source of the Kondyor Pt-mineralisation then had a maximum $^{186}Os/^{188}Os$ of 0.1198303. If we consider such an initial $^{186}Os/^{188}Os$ composition, the D-S2 Pt-alloy would require 242.6 Myr to evolve to its present day $^{186}Os/^{188}Os$ signature. This age is similar within error to that extrapolated from the multi-grain Pt-Os isochron-like trend defined by our Kondyor Pt-alloys (249.8 ± 12 Ma; Fig. 2b).

Ages of ~250-240 Ma are recognised regionally within the Aldan Shield (Lena and Aldan (Palaeo) Rivers: Wang *et al.*, 2011; Miller *et al.*, 2013), the Baikal Lake Region (*e.g.*, Gladkochub *et al.*, 2010) and within basins (*e.g.*, Onon and Mohe-Upper Amur), located South of the Aldan Shield and adjacent to the Mongol-Okhotsk Fold belt (Guo *et al.*, 2017). The Mongol-Okhotsk fold belt (Fig. S-1), which rims the Siberian Craton on its South Margin over *ca*. 3000 km, represents the suture zone left after the closure of the Mongol-Okhotsk Ocean - as its seafloor was subducted under the Siberia craton and under the Mongolia-North China continent (Amur plate) -, and the subsequent collision of the Siberian craton with the Mongolia-North China continent (*e.g.*, Zorin, 1999; Guo *et al.*, 2017). The age distribution along the Mongol-Okhotsk fold belt demonstrates an eastward zip-like closure of the Mongol-Okhotsk ocean (Zorin, 1999) initiated in the Late Palaeozoic in NE Mongolia (Zhao *et al.*, 2017) and in the Early Triassic in the eastern part of the Mongol-Okhotsk belt, south of Aldan Shield Region (Guo *et al.*, 2017). The age of the subsequent collision between the Mongolia-North China continent and Siberia craton also evolves eastwards from Middle Jurassic to Early Cretaceous (Zorin, 1999).

Why are the ^{190}Pt-^{186}Os and the ^{190}Pt-^{4}He "Ages" of the Kondyor Pt-alloys Different?

Both the ^{190}Pt-^{4}He and ^{190}Pt-^{186}Os isotopic systems are based on the radioactive alpha decay of the ^{190}Pt so they should yield identical ages. However, for the Kondyor Pt-alloys, the Pt-He isochronal ages (Shukolyukov *et al.*, 2012a; Mochalov *et al.*, 2016, 2018) are ~110-140 Myr younger than the Pt-Os ages.

Several lines of evidence suggest that the age inconsistency may reflect an open system behaviour of the Pt-He isotopic system. First, Shukolyukov *et al.* (2012a,b) and Mochalov *et al.* (2016) argued that radiogenic ^{4}He is retained in the structure of native metals as vesicles that are only released upon melting of the native metals (>1000 °C). However, the only ^{4}He thermal desorption experiment conducted on Pt-alloys by Shukolyukov *et al.* (2012a) revealed ^{4}He loss ($[^{4}He] \neq 0$) for temperatures as low as ~700 °C (see Fig. 4 in Shukolyukov *et al.*, 2012a). While the ^{4}He loss appears marginal during their experiment, it will be significant if Pt-alloys reside in the lithospheric mantle (with an equilibration temperature >700 °C) for 10s-100s of Myr. It is thus possible that the ^{4}He is not fully trapped in the structure of the Pt-alloys until the ^{4}He closure temperature in these minerals is attained. One can additionally consider how the nanoscale exsolution patterns within the Kondyor Pt-alloys will affect the ^{4}He loss/retention. The grain boundaries proposed as a preferential sink for ^{4}He (Shukolyukov *et al.*, 2012b) may turn out to be preferential ^{4}He

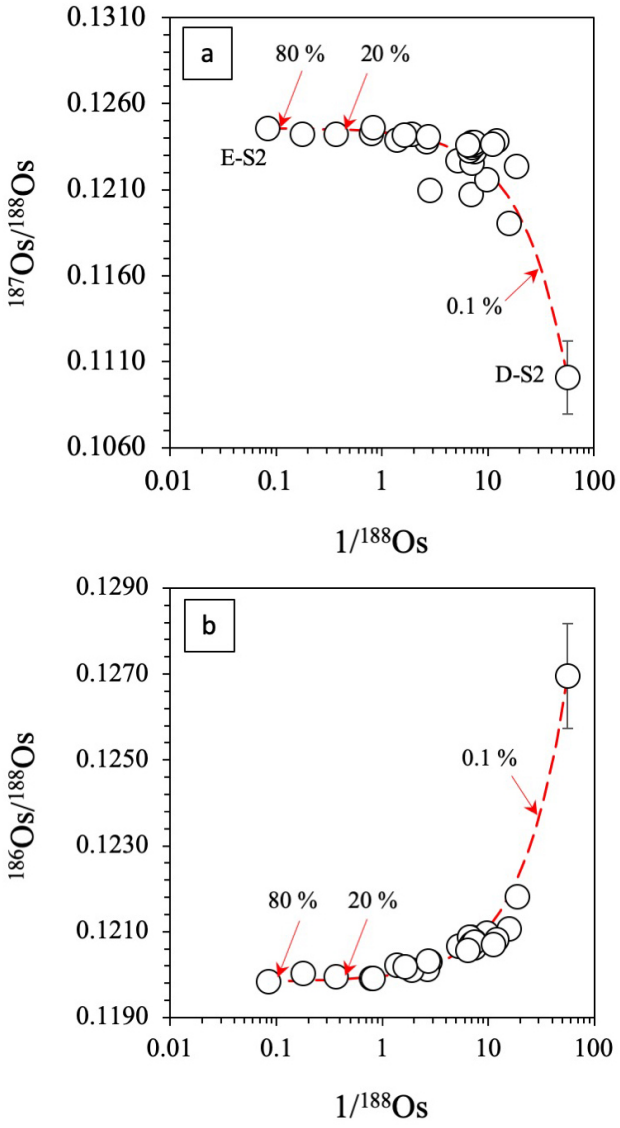

Figure 3 **(a)** $^{186}Os/^{188}Os$ and **(b)** $^{187}Os/^{188}Os$ variations with the Os concentrations ($1/^{188}Os$ beam). Red dotted line represents the overprinting of the most pristine Pt-alloy D-S2 by an Os-rich contaminant characterised by $^{187}Os/^{188}Os$ and $^{186}Os/^{188}Os$ signatures of Pt-alloy E-S2 (0.12457 and 0.119851, respectively).

loss sites when Pt-alloys are intensely exsolved (Fig. 1). The Pt-free nature of the Os exsolution lamellae combined with the extremely Os-poor composition of their Pt-alloy hosts (Fig. 1; Malitch and Thalhammer, 2002; Nekrasov *et al.*, 2005) argues for an equilibration temperature below 500 °C (see Pt-Os phase diagram in Okrugin, 2002), thus well below the 700 °C temperature mark of ^{4}He loss onset observed for Pt alloys (see above). The last evidence suggesting a low closure temperature (<600 °C) of the Pt-He isotopic system comes from the similarity of the Pt-He isochronal ages with the Rb-Sr, Sm-Nd and K-Ar obtained on whole-rock and single minerals (biotite, feldspar) of the dunitic core, pyroxenites and late metasomatic dikes of Kondyor ZUC (149-83 Ma: *e.g.*, Orlova, 1992; Cabri *et al.*, 1998; Pushkarev *et al.*, 2002).

Implication for the Origin and Evolution of the Kondyor ZUC

The combined LA-MC-ICPMS investigation of the Re-Os and Pt-Os isotope signatures demonstrates that the Pt-mineralisation, contemporaneous to the formation of the Kondyor ZUC, originates ~250-240 Myr ago from the melts and fluids produced by partial melting of possibly an Archean PUM-like mantle source, which could be the Siberian cratonic mantle. Considering the orthopyroxene-poor, olivine- and clinopyroxene-rich nature of Kondyor ZUC (Orlova, 1992; Malitch and Thalhammer, 2002) and its extreme Pt-mineralisation, we argue that, rather than being a metasomatised mantle diapir (Burg *et al.*, 2009), Kondyor ZUC represents the root of a ~250-240 Ma old alkaline picritic volcano (Simonov *et al.*, 2011), which together with other Aldan ZUC (*e.g.*, Chad) likely formed part of an Early Triassic island arc at the south-east margin of the Aldan shield due to the subduction of the Mongol-Okhotsk ocean seafloor northwards under the Siberian Craton (see Zorin, 1999; Guo *et al.*, 2017). The uplift associated with the Early Cretaceous collision of the Siberian craton with the Mongolia-North China continent (after the closure of the Mongol-Okhotsk ocean) combined with the subsequent major extensional phase evidenced by the development of Early Cretaceous rift systems may have contributed to the unroofing and exhumation of deep-seated structures such as metamorphic core complexes (Zorin, 1999). In such an unroofing and exhumation scenario, the Kondyor ZUC would attain sub-surface conditions and cool down below the closure temperatures of the K-Ar, Rb-Sr and Pt-He isotope systems, explaining why these geochronometers yield almost exclusively Early to Late Cretaceous ages for the Kondyor ZUC.

Acknowledgements

AL and CB thank the Deutsche Forschungsgemeinschaft for supporting this project (LU 1603/5-1, CB 964/36-1) and EP acknowledges the Russian State Scientific programme No AAAA-A18-118051190022-4. We gratefully thank two anonymous reviewers and our editor, Cin-Ty Lee, for their insightful comments and suggestions.

Editor: Cin-Ty Lee

Additional Information

Supplementary Information accompanies this letter at http://www.geochemicalperspectivesletters.org/article1924.

Cite this letter as: Luguet, A., Nowell, G.M., Pushkarev, E., Ballhaus, C., Wirth, R., Screiber, A., Gottmann, I. (2019) ^{190}Pt-^{186}Os geochronometer reveals open system behaviour of ^{190}Pt-^{4}He isotope system. *Geochem. Persp. Let.* 11, 44–48.

References

Begemann, F., Ludwig, K.R., Lugmair, G.W., Min, K., Nyquist, L.E., Patchett, P.J., Renne, P.R., Shih, C.-Y., Villa, I.M., Walker, R.J. (2001) Call for an improved set of decay constants for geochronological use. *Geochimica et Cosmochimica Acta* 65, 111-121.

Burg, J.-P., Bodinier, J.-L., Gerya, T., Bedini, R.-M., Boudier, F., Dautria, J.-M., Prikhodko, V., Efimov, A., Pupier, E., Balanec, J.-L. (2009) Translithospheric Mantle Diapirism: Geological Evidence and Numerical Modelling of the Kondyor Zoned Ultramafic Complex (Russian Far-East). *Journal of Petrology* 50, 289-321.

Cabri, L.J., Stern, R.A., Czamanske, G.K. (1998) Osmium isotope measurements of the Pt-Fe alloy placer nuggets from the Konder Intrusion using a Shrimp II Ion Microprobe. *8th International Platinum Symposium Abstracts*, 55-58.

Coggon, J.A., Nowell, G.M., Pearson, D.G., Oberthür, T., Lorand, J.-P., Melcher, F., Parman, S.W. (2012) The ^{190}Pt-^{186}Os decay system applied to dating platinum-group element mineralization of the Bushveld Complex, South Africa. *Chemical Geology* 302-303, 48-60.

Davies, G.R., Stolz, A.J., Mahotkin, I.L., Nowell, G.M., Pearson, D.G. (2006) Trace element and Sr-Pb-Nd-Hf isotope evidence for ancient, fluid-dominated enrichment of the source of Aldan shield lamproites. *Journal of Petrology* 47, 1119-1146.

Day, J.M.D., Walker, R.J., Warren, J.M. (2017) ^{186}Os-^{187}Os and highly siderophile element abundance systematics of the mantle revealed by abyssal peridotites and Os-rich alloys. *Geochimica et Cosmochimica Acta* 200, 232-254.

Gladkochub, D.P., Donskaya, T.V., Ivanov, A.V., Ernst, R., Mazukabzov, A.M., Pisarevsky, S.A., Ukhova, N.A. (2010) Phanerozoic mafic magmatism in the southern Siberian craton: geodynamic implications. *Russian Geology and Geophysics* 51, 952–964.

Guo, Z-X., Yang, Y-T., Zyabrev, S., Hou, Z-H. (2017) Tectonostratigraphic evolution of the Mohe-Upper Amur Basin reflects the final closure of the Mongol-Okhotsk Ocean in the latest Jurassic-earliest Cretaceous. *Journal of Asian Earth Sciences* 145, 494-511.

Ionov, D.A., Shirey, S.B. Weiss, D., Brügmann G. (2006) Os–Hf–Sr–Nd isotope and PGE systematics of spinel peridotite xenoliths from Tok, SE Siberian craton: Effects of pervasive metasomatism in shallow refractory mantle. *Earth and Planetary Science Letters* 241, 47-64.

Malitch, K.N., Thalhammer, O.A.R. (2002) Pt–Fe nuggets derived from clinopyroxenite–dunite massifs, Russia: a structural, compositional and osmium-isotope study. *The Canadian Mineralogist* 40, 395-418.

Meibom, A., Frei, R. (2002) Evidence for an Ancient Osmium Isotopic Reservoir in Earth. *Science* 296, 516-518.

Meisel, T., Walker, R.J., Irving, A.J., Lorand, J.-P. (2001) Osmium isotopic compositions of mantle xenoliths: A global perspective. *Geochimica et Cosmochimica Acta* 65, 1311-1323.

Miller, E.L., Soloviev, A.V., Prokopiev, A.V., Toro, J., Harris, D., Kuzmichev, A.B., Gehrels, G.E., (2013) Triassic river systems and the paleo-Pacific margin of northwestern Pangea. *Gondwana Research* 23, 1631-1645.

Mochalov, A.G., Yakubovich, O.V., Bortnikov, N.S. (2016) ^{190}Pt-^{4}He Age of PGE Ores in the Alkaline-Ultramafic Kondyor Massif (Khabarovsk District, Russia). *Doklady Earth Sciences* 469, 846–850.

Mochalov, A.G., Yakubovich, O.V., Zolotarev, A.A. (2018) Structural Transformations and Retention of Radiogenic ^{4}He in Platinum Minerals under Mechanical Deformations. *Doklady Earth Sciences* 480, 591–594.

Nekrasov, I.Y., Lennikov, A.M., Zalishchak, B.L., Oktyabrsky, R.A., Ivanov, V.V., Sapin, V.I., Taskaev, V.I. (2005) Composition variations in platinum-group minerals and gold, Konder alkaline-ultrabasic massif, Aldan Shield, Russia. *The Canadian Mineralogist* 43, 637-654.

Okrugin, A.V. (2002) Phase transformations and genesis of platinum-group minerals in various types of platinum-bearing deposits. In: Boudreau, A.E. (Ed.) *9th International Platinum Symposium (Billings), Extended Abstracts.* Duke University Press, Durham, North Carolina, 349-353.

Orlova, M.P. (1992) Geology and genesis of the Konder Massif. *Geology of the Pacific Ocean* 8, 120-132.

Pearson, D.G., Parman, S.W., Nowell, G.M. (2007) A link between large mantle melting events and continent growth seen in osmium isotopes. *Nature* 449, 202-205.

Pushkarev, Yu.D., Kostoyanov, A.I., Orlova, M.P., Bogomolov, E.S. (2002) Peculiarities of the Rb-Sr, Sm-Nd, Re-Os and K-Ar isotope systems in the Kondyor massif: mantle substratum, enriched by PGE. *Regional Geology and Metallogeny* 16, 80-91 (in Russian).

Pushkarev, E.V., Kamenetsky, V.S., Morozova, A.V., Khiller, V.V., Glavatskykh, S.P., Rodemann, T. (2015) Ontogeny of Ore Cr-spinel and composition of inclusions as indicators of the Pneumatolytic-Hydrothermal Origin of PGM-bearing Chromitites from Kondyor Massif, The Aldan Shield. *Geology of Ore Deposits* 57, 352-380.

Shukolyukov, Yu.A., Yakubovich, O.V., Mochalov, A.G., Kotov, A.B., Sal'nikova, E.B., Yakovleva, S.Z., Korneev, S.I., Gorokhovskii, B.M. (2012a) New Geochronometer for the Direct Isotopic Dating of Native Platinum Minerals (^{190}Pt-^{4}He Method). *Petrology* 20, 491-507.

Shukolyukov, Yu.A., Yakubovich, O.V., Yakovleva, S.Z., Sal'nikova, E.B., Kotov, A.B., Rytsk, E.Yu (2012b) Geothermochronology based on noble gases: III. Migration of radiogenic He in the crystal structure of native metals with applications to their isotopic dating. *Petrology* 20, 1-20.

Simonov, V.A., Prikhod'ko, V.S., Kovyazin, S.V. (2011) Genesis of Platiniferous Massifs in the Southeastern Siberian Platform. *Petrology* 19, 549-567.

Walker, R.J., Morgan, J.W., Beary, E.S., Smoliar, M.I., Czamanske, G.K., Horan, M.F. (1997) Applications of the ^{190}Pt-^{186}Os isotope system to geochemistry and cosmochemistry. *Geochimica et Cosmochimica Acta* 61, 4799-4807.

Wang, C.Y., Campbell, I.H., Stepanov, A.S., Allen, C.M., Burtsev, I.N. (2011) Growth rate of the preserved continental crust: II. Constraints from Hf and O isotopes in detrital zircons from Greater Russian Rivers. *Geochimica et Cosmochimica Acta* 75, 1308-1345.

Zhao, P., Xu, B., Jahn, B.-M. (2017) The Mongol-Okhotsk Ocean subduction-related Permian peraluminous granites in northeastern Mongolia: constraints from zircon U-Pb ages, whole-rock elemental and Sr-Nd-Hf isotopic compositions. *Journal of Asian Earth Sciences* 144, 225-240.

Zorin, Y.A. (1999) Geodynamics of the western part of the Mongolia–Okhotsk collisional belt, Trans-Baikal region (Russia) and Mongolia. *Tectonophysics* 306, 33-56.

Geochemical Perspectives Letters

^{190}Pt-^{186}Os geochronometer reveals open system behaviour of the ^{190}Pt-^{4}He isotope system

A. Luguet, G.M. Nowell, E. Pushkarev, C. Ballhaus, R. Wirth, A. Schreiber, I. Gottman

Supplementary Information

The Supplementary Information includes:

- 1. The Kondyor Zoned Ultramafic Complex (ZUC)
- 2. The Pt-alloys of the Kondyor ZUC and the Origin of their Pure Os Exsolution Lamellae
- 3. Methods
- Figure S-1
- Tables S-1 and S-2
- Supplementary Information References

1. The Kondyor Zoned Ultramafic Complex (ZUC)

The Kondyor ZUC is a circular, crater-like structure (*ca*. 6 km in diameter) having intruded the Archean basement and Proterozoic metasedimentary rocks of the Aldan Shield, on the SE edge of the Siberian Craton (*e.g*., Shcheka *et al*., 2004; Burg *et al*., 2009; Simonov *et al*., 2010) (Fig. S-1). Its zoned structure consists in a dunite core, the dominant rock type, surrounded by successive irregular shells of pyroxenites-wehrlites and gabbros and cross-cut in its SW part by numerous dykes of glimmerite, phlogopite-amphibole-apatite-carbonate and Fe-Ti-oxide bearing pyroxenites and magnetite-bearing clinopyroxenites (*e.g*., Burg *et al*., 2009). The platinum group minerals, namely Pt-alloys, are mostly associated with dm-sized chromite pods in the dunite. They render Kondyor one of the world's largest alluvial Pt deposits.

Neither the origin of the Kondyor ZUC (mantle intrusion at the apex of a mantle diapir; Burg *et al*., 2009 *vs*. fractional crystallisation of magma, see Simonov *et al*., 2010; Chaika and Izokh, 2018 for the Inagli Aldan ZUC) nor the age of the Pt mineralisation and the overall timeline of the Kondyor ZUC evolution are firmly constrained. Numerous investigations using the K-Ar, Rb-Sr, Sm-Nd isotopic systems on dunites, metasomatised dunites (*i.e*. phlogopite bearing), metasomatic pyroxenites-gabbros-syenites and late dykes at the whole-rock and mineral scales (*e.g*., phlogopite, clinopyroxene) indicate ages between 149-83 Ma (Orlova, 1992; Kononova *et al*., 1995; Pushkarev *et al*., 2002; Savatenkov and Mochalov, 2018), which are encompassing the "isochronal" ^{190}Pt-^{4}He age obtained on Pt-alloys (112 ± 7 Ma and 129 ± 6 Ma: Shukolyukov *et al*., 2012; Mochalov *et al*., 2016 respectively). In contrast, oval and rounded zircons from the dunitic core recorded Paleoproterozoic to Archean ages (1885 ± 52 and 2477 ± 18 Ma) (Malitch *et al*., 2012). Re-Os T_{RD} model ages obtained on (i) Pt-alloys and (ii) Os-alloys, erlichmanite (OsS_2), sperrylite ($PtAs_2$) associated with the Pt-alloys, collected from both the dunite-hosted chromitites and the placer deposit, point at Neoproterozoic (603-658 Ma) to future ages (Cabri *et al*., 1998; Malitch and Thalhammer, 2002) when back-calculated to the upper mantle ^{187}Os/^{188}Os estimate of Meisel *et al*. (2001).

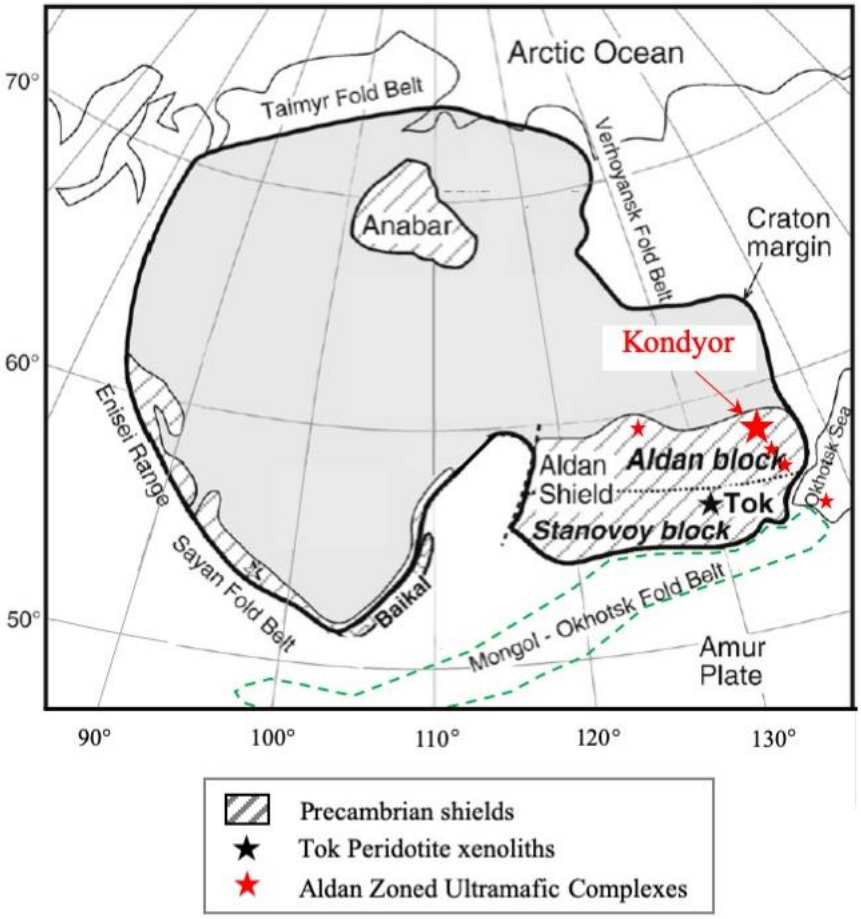

Figure S-1 Sketch map of the Siberian craton, the Aldan Shield and adjacent fold belts (modified from Tommasi *et al*., 2008).

2. The Pt-Alloys of the Kondyor ZUC and the Origin of their Pure Os Exsolution Lamellae

The Platinum Group Minerals of the Kondyor ZUC have been the focus of detailed investigations such as those of Malitch and Thalhammer (2002), Shcheka *et al*. (2004) and Nekrasov *et al*. (2005). The spectrum of Kondyor PGM is very wide consisting predominantly of Pt-alloys, mainly Pt_3Fe, with subordinate occurrences of Os±Ir±Ru alloys, sulfides of Highly Siderophile Elements (*e.g.*, laurite RuS_2, malanite $Cu(Pt, Ir)_2S_4$) and Pd-Pt compounds such as arsenides, tellurides, bismuthides and antimonites. The $^{190}Pt/^{188}Os$ and $^{187}Re/^{188}Os$ of our subset of Pt-alloys suggest that these Pt-alloys contain 10s ppm to wt. % Os and <100 ppb Re. Interestingly, the FIB-TEM investigations we conducted on a few grains revealed a very complex nanoscale exsolution pattern consisting of spinodal exsolutions of Pt-Fe alloys (*e.g.*, Pt_3Fe, PtFe) and pure Os exsolution lamellae (Fig. 1). Such nanoscale exsolution patterns were already observed by Malitch and Thalhammer (2002) and Shcheka *et al*. (2004).

Malitch and Thalhammer (2002) proposed that this mineralogical assemblage reflected a fractional crystallisation sequence starting at high temperature, low fS_2 conditions with the crystallisation of the Pt-Fe alloys, followed upon cooling and increasing fS_2-fO_2 by the exsolution of the Os lamellae, and the formation at lower temperature of the As, Te, Bi, Sn, Au, Cu, Pd, Pt compounds. Namely, the large Pt-alloys showing enrichments in Au-Ag-Cu-S-Sn-Sb-Bi-Te may have formed in a pegmatitic environment (*i.e.*, NaCl-rich solution) possibly generated when the residual liquids became fluid-saturated (Shcheka *et al*., 2004).

The $^{187}Os/^{188}Os$ signatures of the Kondyor Pt-alloys we obtained by LA-MC-ICPMS and especially their negative relationship with the $^{187}Re/^{188}Os$ ratios provide further insights into their origin(s) and the evolution of the Pt-mineralisation as a whole. The most unradiogenic $^{187}Os/^{188}Os$ composition of the Kondyor Pt-alloys (0.110096; grain D-S2), is obtained for the Os-poorest and Pt-

richest alloy (see ^{188}Os and $^{190}Pt/^{188}Os$: Table S-2) and reveals that the source of the Pt-mineralisation is likely an Archean mantle reservoir. In contrast, all the other analyses, which are clearly richer in Os, likely sampled a higher proportion of Os lamellae. These yield a much higher $^{187}Os/^{188}Os$ reaching up to ~0.1246 for the Os-richest alloy (grain E-S2). Considering the fractional crystallisation sequence proposed by Malitch and Thalhammer (2002), upon exsolution, the Os lamellae and their Pt-alloy hosts would have the same $^{187}Os/^{188}Os$ isotopic composition. Therefore, the most radiogenic $^{187}Os/^{188}Os$ of the Os exsolution-rich Pt-alloy (alloy E-S2) can only be explained due to ^{187}Os in-growth since the early Triassic mineralisation process if its Re/Os ratio is around 0.73 ($^{187}Re/^{188}Os$ ~ 3.5). Such a Re-rich composition is not supported by the EDS spectra of the Os exsolution lamellae (Fig. 1), nor by the $^{187}Re/^{188}Os$ ratios determined by LA-MC-ICPMS, nor the experimental investigations on Re and Os partitioning in HSE alloys of Fonseca *et al*. (2017). In fact, from both the natural PGM (see Walker *et al*., 1997; Meibom and Frei, 2002; Nowell *et al*., 2008b; Coggon *et al*., 2011; Wainwright *et al*., 2016) and experimental (Fonseca *et al*., 2017) viewpoints, it is expected that upon exsolution of pure Os lamellae from a Pt-alloy, the Re will partition preferentially into the Pt-Fe alloy while the Os will partition preferentially into the Os-alloys. Therefore, with ^{187}Os ingrowth, the more radiogenic $^{187}Os/^{188}Os$ signatures should develop within the Pt-Fe alloys, while the pure Os lamellae would be characterised by a lower, typically unradiogenic $^{187}Os/^{188}Os$ signature.

The Os-rich Pt-alloys (such as point E-S2) and the Os-poor Pt-alloy (grain D-S2), which can be found associated on the microscale within one single alloy grain (DS-1 and D-S2 in alloy grain D) represent thus different alloy generations or growth phases derived from mantle sources compositionally distinct. The shift from an Archean mantle source for the Os-poor Pt alloys to that of a mantle source characterised by a more radiogenic $^{187}Os/^{188}Os$ signatures for the Os-rich Pt-alloy, likely reflects the gradual overprinting of the Siberian cratonic mantle by subduction components over the ca. 100 millions years that the subduction of the Mongol-Okhotsk ocean seafloor lasted. The gradual overprinting by subduction components, namely fluids, is supported by the negative trend between $^{187}Os/^{188}Os$ *vs*. $^{187}Re/^{188}Os$ and the possible growth in pegmatitic environment of part of the PGM mineralogical assemblage suggested by Shcheka *et al*. (2004). The Kondyor Pt-alloys then possibly constitute an example where the overprinting event affected the mantle source of the Pt-mineralisation rather than purely affecting the alloys (*via* contamination and recrystallisation).

Such an alternative scenario for the evolution of the Kondyor Pt-alloys however requires to be firmly constrained by a thorough investigation at the micro to nanometric scale of the composition and isotopic signatures of the Os exsolution lamellae and their Pt-alloy hosts.

3. Methods

The simultaneous determination of the $^{187}Os/^{188}Os$ and $^{186}Os/^{188}Os$ signatures was performed by LA-MC-ICPMS using the New Wave UP213 nano-second laser system coupled with a Thermo-Finnigan Neptune MC-ICPMS of the Arthur Holmes Isotope Geology Laboratory at the Department of Earth Sciences of Durham, UK. The full details of the analytical procedure and data reduction are provided in Nowell *et al*. (2008b). Still, for the analytical session of the Kondyor Pt-alloys, the conditions of the laser system were specifically set to 20 Hz frequency, 100 % power and a 130 μm beam diameter. These laser conditions were kept constant throughout the analytical session allowing us to use the ^{188}Os signal as a proxy of the relative Os concentrations of the Kondyor alloys. Since the Kondyor alloys are Pt-rich and Os-poor, the mass bias correction for the whole analytical session was performed using the $^{189}Os/^{188}Os$ ratio (1.21978), as ^{189}Os is free from direct Pt interferences at the opposite of ^{192}Os or ^{190}Os.

The precision and accuracy of $^{186}Os/^{188}Os$ and $^{187}Os/^{188}Os$ ratios and the efficiency of the ^{187}Re and ^{186}W interference correction on the radiogenic ^{187}Os and ^{186}Os isotopes were estimated by measuring repetitively 1ppm DROsS standard solutions pure and variably doped in Re and W (by solution MC-ICPMS) as well as the Durham in-house Os-rich alloy standard (alloy grain 36720G3) (measured by LA-MC-ICPMS). The reproducibilities of the $^{186}Os/^{188}Os$ and $^{187}Os/^{188}Os$ compositions of the DROsS solutions (n=11, pure and, W- and Re-doped solutions) are respectively 96 ppm and 135 ppm. The $^{187}Os/^{188}Os$ variations are observed among as well as within the analyses of the pure, and of each of the W- and Re-doped solutions. These variations are then independent of the Re signal intensities, demonstrating that they do not result from a ^{187}Re interference correction issue. The reproducibility of the DROsS $^{186}Os/^{188}Os$ ratios improves significantly (33 ppm) when the analyses #1 and #2 from the pure DROsS solution are omitted. This combined to the absence of correlation between the ^{182}W beam intensity, the $^{182}W/^{188}Os$ and the $^{186}Os/^{188}Os$ demonstrates the robustness of the W-correction applied to W-bearing samples, with $^{182}W/^{188}Os$ ratios of up to 0.17 as seen for the 1ppm DROsS solution doped with 0.1 ppm W + 0.05 ppm Re. The Kondyor Pt-alloys show much lower $^{182}W/^{188}Os$ ratios (0.000004-0.0026), intermediate between those of the pure 1 ppm DROsS solution and the 1ppm solution doped with 0.05 ppm W and 0.01 ppm Re, for which the ^{186}W interference correction is robust.

Overall, our average DROsS $^{186}Os/^{188}Os$ and $^{187}Os/^{188}Os$ ratios differ by 207 ppm and 69 ppm when compared with those obtained on the pure 1 ppm DROsS standard solution (2.5 ppm) of Nowell *et al*. (2008a), and by 141 and 38 ppm when compared

with those obtained on the pure DROsS standard solution (0.2 ppm) of Nowell *et al*. (2008b). For the Durham in-house Os-rich alloy standard (alloy grain 36720G3), the $^{186}Os/^{188}Os$ and $^{187}Os/^{188}Os$ differ respectively by 195 ppm and 293 ppm when compared to the analyses of Nowell *et al*. (2008b) (see Table S-1) and show reproducibilities of 146 and 149 ppm respectively. The lower precision and accuracy obtained on the DROsS solutions and the alloy grain 36720G3 during the Kondyor analytical session most likely result from different analytical conditions (e.g., lower signal intensity by a factor 3.8 to 7.4). While these deviations are significant when the range of the $^{186}Os/^{188}Os$ signatures for the Earth's mantle is taken into consideration ($^{186}Os/^{188}Os$ variation of 95 ppm for ca. 3.5 Gyr), it is important to highlight that the range of $^{186}Os/^{188}Os$ and $^{187}Os/^{188}Os$ in the Kondyor Pt-alloys are 2-4 orders of magnitude larger than the precisions and accuracies estimated on our standard solutions and in-house standard Os-rich alloy.

Similarly to the procedure adopted in other publications investigating the $^{186}Os/^{188}Os$ of mantle samples (see Day *et al*., 2017), we have normalised our Kondyor Pt-alloys $^{186}Os/^{188}Os$ and $^{187}Os/^{188}Os$ ratios to the $^{186}Os/^{188}Os$ and $^{187}Os/^{188}Os$ ratios of standard materials in order to erase possible analytical bias. In doing so, we considered first the deviation between our average DROsS values obtained during the Kondyor analytical session and those determined on the 2.5 ppm DROsS solution by Nowell *et al*. (2008a). Importantly, all DROsS values used for this first normalisation are mass bias corrected using the $^{189}Os/^{188}Os$ ratios (1.21978) and measured by solution MC-ICPMS. We conducted a second normalisation as the interpretation of the $^{186}Os/^{188}Os$ and $^{187}Os/^{188}Os$ signatures of Kondyor Pt-alloys requires comparison to the $^{186}Os/^{188}Os$ and $^{187}Os/^{188}Os$ signatures of the primitive mantle (Day *et al*., 2017), these latter were estimated from TIMS analyses using $^{192}Os/^{188}Os$ as mass bias monitor. Such normalisation between TIMS, solution MC-ICPMS and LA-MC-ICPMS data and for different mass bias monitors is possible thanks to the extensive investigations performed on the $^{186}Os/^{188}Os$ and $^{187}Os/^{188}Os$ analytical procedure by Luguet *et al*. (2008-TIMS) and Nowell *et al*. (2008a, b-solution and LA-MC-ICPMS respectively), for which four standard solutions - available to cross-check the precision and accuracy of Os isotope measurements between laboratories - have been repetitively measured. This second normalisation is based on the deviations of the $^{186}Os/^{188}Os$ and the $^{187}Os/^{188}Os$ ratios for the UMd standard solution between the values obtained (i) by Nowell *et al*. (2008a) using solution-MC-ICPMS and $^{189}Os/^{188}Os$ for the bias correction and those determined by (ii) Day *et al*. (2017) using TIMS and $^{192}Os/^{188}Os$ for the mass bias correction.

These 2-fold normalisations only modify the values of the $^{186}Os/^{188}Os$ and $^{187}Os/^{188}Os$ signatures but do not alter any relationships that may exist between for example $^{190}Pt/^{188}Os$ and $^{186}Os/^{188}Os$ (*i.e.* isochron) or between $^{186}Os/^{188}Os$ vs. $^{187}Os/^{188}Os$. Finally, it is important to note that while this 2-fold normalisation of the $^{186}Os/^{188}Os$ and $^{187}Os/^{188}Os$ ratios allows for a direct comparison of datasets obtained by different laboratories using different analytical approaches and data reduction procedures (*i.e.* mass bias correction), the values of the $^{186}Os/^{188}Os$ and the $^{187}Os/^{188}Os$ obtained or normalised to match those obtained by TIMS may be slightly overestimated as the TIMS $^{186}Os/^{188}Os$ and $^{187}Os/^{188}Os$ data suffer from residual interferences (see Luguet *et al*., 2008).

Supplementary Tables

Table S-1 ^{188}Os, ^{182}W and ^{185}Re signal intensities and Os isotope compositions for the DROsS reference solution (Solution MC-ICPMS) and the Durham in-house Os-alloy standard 36720G3 (LA-MC-ICPMS) analysed during the analytical session of the Kondyor Pt-alloys.

Table S-1 (Part 1)

Analysis	^{188}Os(V)	1se	^{182}W (V)	1se	^{185}Re (V)	1se	$^{187}Re/^{188}Os$	1se
				DROsS solution				
				1 ppm DROsS				
#1	2.537	0.010	0.000034	0.000007	0.000042	0.000006	0.0000325	0.0000034
#2	2.686	0.007	0.000038	0.000004	0.000039	0.000004	0.0000236	0.0000020
#3	2.554	0.010	0.000030	0.000006	0.000042	0.000007	0.0000256	0.0000041
#4	2.546	0.009	0.000033	0.000005	0.000043	0.000006	0.0000265	0.0000033
#5	2.566	0.008	0.000027	0.000006	0.000050	0.000008	0.0000339	0.0000050
average #1-5							*0.000028*	
2 sd							*0.000009*	
				1 ppm DROsS + 0.05 ppm W + 0.01 ppm Re				
#6	2.837	0.009	0.245821	0.000775	0.091415	0.000286	0.055211	0.000006
#7	2.826	0.011	0.244571	0.000965	0.091062	0.000359	0.055204	0.000006
#8	2.809	0.015	0.243370	0.001305	0.090519	0.000486	0.055213	0.000005
average #6-8							*0.055209*	
2 sd							*0.000010*	
				1 ppm DROsS + 0.1 ppm W + 0.05 ppm Re				
#9	2.671	0.009	0.471057	0.001594	0.419768	0.001428	0.269247	0.000023
#10	2.679	0.009	0.472484	0.001541	0.421045	0.001355	0.269318	0.000019
#11	2.666	0.010	0.470179	0.001718	0.418942	0.001539	0.269295	0.000018
average #9-11							*0.269287*	
2 sd							*0.000073*	
average #1-11								
2 sd								
				Nowell *et al.* (2008a) 2.5 ppm DROsS (n=21)				
average								
2 sd								
				Nowell *et al.* (2008b) 0.2 ppm DROsS (n=5)				
average								
2 sd								
				Durham In-house standard 36720G3 Os-alloy				
#12	1.950	0.063	-0.000006	0.000005	0.001157	0.000029	0.001021	0.000009
#13	2.937	0.071	-0.000003	0.000006	0.001797	0.000054	0.001030	0.000008
#14	1.968	0.055	0.000001	0.000006	0.001273	0.000025	0.001118	0.000014
#15	1.507	0.050	-0.000002	0.000005	0.000931	0.000023	0.001065	0.000012
average #12-15								

2 sd								
Nowell *et al.* (2008b) (n=7)								
average	*11.11*							
2 sd	*2.05*							

Table S-1 (Part 2)

Analysis	$^{190}Pt/^{188}Os$	1se	$^{184}Os/^{188}Os$	1se	$^{186}Os/^{188}Os$	1se	$^{187}Os/^{188}Os$	1se
DROsS solution								
1 ppm DROsS								
#1	0.0000842	0.000050	0.001304	0.000004	0.119920	0.000008	0.160915	0.000006
#2	0.0000472	0.000027	0.001300	0.000002	0.119927	0.000003	0.160925	0.000003
#3	-0.0000473	0.000048	0.001308	0.000004	0.119937	0.000007	0.160927	0.000007
#4	-0.0000547	0.000052	0.001303	0.000003	0.119936	0.000007	0.160942	0.000007
#5	-0.0000324	0.000048	0.001308	0.000003	0.119937	0.000007	0.160924	0.000009
average #1-5	*-0.000001*		*0.001305*		*0.119931*		*0.160927*	
2 sd	*0.000125*		*0.000007*		*0.000015*		*0.000020*	
1 ppm DROsS + 0.05 ppm W + 0.01 ppm Re								
#6	0.000027	0.000048	0.001307	0.000007	0.119939	0.000005	0.160929	0.000006
#7	0.000034	0.000048	0.001314	0.000008	0.119936	0.000007	0.160928	0.000007
#8	-0.000070	0.000048	0.001308	0.000007	0.119937	0.000008	0.160937	0.000006
average #6-8	*-0.000003*		*0.001310*		*0.119937*		*0.160931*	
2 sd	*0.000116*		*0.000008*		*0.000002*		*0.000010*	
1 ppm DROsS + 0.1 ppm W + 0.05 ppm Re								
#9	0.000065	0.000045	0.001309	0.000011	0.119937	0.000010	0.160918	0.000013
#10	-0.000041	0.000052	0.001310	0.000013	0.119932	0.000013	0.160909	0.000012
#11	-0.000012	0.000046	0.001309	0.000009	0.119935	0.000013	0.160944	0.000012
average #9-11	*0.000004*		*0.001309*		*0.119935*		*0.160924*	
2 sd	*0.000110*		*0.000001*		*0.000005*		*0.000036*	
average #1-11	*0.000000*		*0.001307*		*0.119934*		*0.160927*	
2 sd	*0.000107*		*0.000008*		*0.000011*		*0.000022*	
Nowell *et al.* (2008a) 2.5 ppm DROsS (n=21)								
average			*0.001298*		*0.119909*		*0.160916*	
2 sd			*0.000002*		*0.000004*		*0.000004*	
Nowell *et al.* (2008b) 0.2 ppm DROsS (n=5)								
average					*0.119917*		*0.160921*	
2 sd					*0.000020*		*0.000018*	
Durham In-house standard 36720G3 Os-alloy								
#12	0.000277	0.000079	0.001305	0.000005	0.119844	0.000006	0.123950	0.000008
#13	-0.000049	0.000103	0.001301	0.000002	0.119845	0.000008	0.123952	0.000005
#14	0.000197	0.000108	0.001303	0.000004	0.119833	0.000010	0.123962	0.000009
#15	0.000112	0.000076	0.001310	0.000005	0.119827	0.000010	0.123970	0.000009

average #12-15	*0.000134*	*0.001305*	*0.119837*	*0.123958*
2 sd	*0.000279*	*0.000008*	*0.000017*	*0.000018*
Nowell *et al.* (2008b) (n=7)				
average	*0.000130*	*0.001305*	*0.119814*	*0.123922*
2 sd	*0.003280*	*0.000001*	*0.000009*	*0.000013*

Table S-2 ^{188}Os, ^{182}W and ^{185}Re signal intensities and Os isotope compositions of the Kondyor Pt-alloy grains (A to M) analysed by LA-MC-ICPMS.

Table S-2 (Part 1)

Alloy	^{188}Os(V)	1se	^{182}W (V)	1se	^{185}Re (V)	1se	^{187}Re/^{188}Os	1se
A-S1	0.356	0.042	0.000035	0.000006	0.000076	0.000006	0.000483	0.000055
A-S2	0.064	0.002	0.000021	0.000006	0.000049	0.000007	0.001271	0.000174
B-S1	0.145	0.002	0.000034	0.000007	0.000076	0.000005	0.000935	0.000058
B-S2	1.273	0.088	0.000040	0.000006	0.000070	0.000007	0.000100	0.000014
C-S1	0.379	0.022	0.000023	0.000005	0.000060	0.000006	0.000295	0.000029
C-S2	0.103	0.005	0.000033	0.000005	0.000067	0.000006	0.001233	0.000093
D-S1	0.192	0.016	0.000036	0.000006	0.000069	0.000006	0.000709	0.000075
D-S2	0.018	0.003	0.000047	0.000005	0.000035	0.000005	0.005411	0.001269
E-S1	0.142	0.003	0.000051	0.000006	0.000072	0.000006	0.000850	0.000075
E-S2	12.018	1.659	0.000048	0.000007	0.000110	0.000007	0.000046	0.000011
F-S1	0.729	0.145	0.000032	0.000005	0.000086	0.000005	0.000420	0.000051
F-S2	5.651	1.124	0.000069	0.000009	0.000088	0.000008	0.000250	0.000073
G-S1	2.750	0.552	0.000030	0.000005	0.000065	0.000006	0.000188	0.000035
G-S2	0.135	0.002	0.000027	0.000005	0.000057	0.000006	0.000677	0.000074
H-S1	0.150	0.008	0.000037	0.000005	0.000082	0.000006	0.000971	0.000082
H-S2	0.143	0.010	0.000036	0.000005	0.000071	0.000007	0.000910	0.000100
I-S1	0.526	0.048	0.000037	0.000004	0.000081	0.000008	0.000332	0.000037
I-S2	0.054	0.001	0.000024	0.000006	0.000076	0.000005	0.002320	0.000152
J-S1	0.135	0.002	0.000022	0.000006	0.000064	0.000006	0.000731	0.000059
J-S2	0.370	0.043	0.000041	0.000006	0.000069	0.000008	0.000424	0.000057
K-S1	0.143	0.001	0.000029	0.000005	0.000051	0.000006	0.000675	0.000067
K-S2	0.148	0.002	0.000043	0.000005	0.000059	0.000006	0.000722	0.000072
K-S3	0.136	0.002	0.000076	0.000053	0.000046	0.000006	0.000617	0.000079
K-S4	0.156	0.003	0.000042	0.000005	0.000067	0.000006	0.000759	0.000057
L-S1	0.083	0.002	0.000015	0.000006	0.000051	0.000006	0.000893	0.000108
L-S2	1.221	0.088	0.000016	0.000006	0.000044	0.000006	0.000069	0.000011
M-S1	0.616	0.156	0.000120	0.000071	0.000057	0.000007	0.000402	0.000073
M-S2	0.090	0.002	0.000022	0.000006	0.000044	0.000006	0.000793	0.000117

Table S-2 (Part 2)

Alloy	^{190}Pt/^{188}Os	1se	^{184}Os/^{188}Os	1se	^{186}Os/^{188}Os	1se	^{187}Os/^{188}Os	1se
A-S1	1.42	0.11	0.001358	0.000029	0.120311	0.000051	0.120969	0.000269
A-S2	3.16	0.10	0.001201	0.000128	0.121065	0.000139	0.119044	0.000283
B-S1	2.57	0.05	0.001447	0.000056	0.120872	0.000085	0.120758	0.000122
B-S2	0.28	0.03	0.001295	0.000009	0.119922	0.000018	0.124286	0.000060
C-S1	0.82	0.04	0.001336	0.000021	0.120138	0.000032	0.123799	0.000055
C-S2	3.13	0.08	0.001417	0.000081	0.120970	0.000079	0.121587	0.000138

D-S1	2.32	0.19	0.001331	0.000045	0.120668	0.000073	0.122697	0.000176
D-S2	19.89	2.07	0.001996	0.000949	0.126959	0.001221	0.110096	0.002136
E-S1	2.79	0.05	0.001302	0.000044	0.120778	0.000055	0.122572	0.000097
E-S2	0.06	0.04	0.001307	0.000005	0.119852	0.000018	0.124577	0.000026
F-S1	1.17	0.14	0.001366	0.000022	0.120221	0.000042	0.123925	0.000090
F-S2	0.76	0.21	0.001309	0.000038	0.120037	0.000080	0.124251	0.000123
G-S1	0.66	0.10	0.001288	0.000015	0.119953	0.000039	0.124261	0.000059
G-S2	2.58	0.05	0.001433	0.000065	0.120789	0.000062	0.123240	0.000101
H-S1	2.68	0.12	0.001400	0.000060	0.120886	0.000086	0.123263	0.000101
H-S2	2.59	0.16	0.001290	0.000065	0.120692	0.000093	0.123453	0.000117
I-S1	0.85	0.06	0.001313	0.000015	0.120122	0.000031	0.124259	0.000048
I-S2	5.22	0.11	0.001130	0.000145	0.121829	0.000132	0.122365	0.000243
J-S1	2.26	0.04	0.001418	0.000052	0.120637	0.000066	0.123605	0.000085
J-S2	1.47	0.12	0.001325	0.000041	0.120317	0.000061	0.124083	0.000068
K-S1	2.29	0.04	0.001448	0.000045	0.120737	0.000063	0.123759	0.000076
K-S2	2.22	0.03	0.001313	0.000059	0.120676	0.000044	0.123641	0.000071
K-S3	2.34	0.03	0.001455	0.000055	0.120765	0.000057	0.123743	0.000092
K-S4	2.40	0.05	0.001331	0.000048	0.120575	0.000060	0.123616	0.000070
L-S1	2.70	0.06	0.001522	0.000103	0.120823	0.000096	0.123837	0.000121
L-S2	0.23	0.02	0.001317	0.000010	0.119925	0.000018	0.124602	0.000015
M-S1	1.11	0.11	0.001336	0.000039	0.120186	0.000055	0.124199	0.000093
M-S2	2.53	0.11	0.001331	0.000080	0.120703	0.000116	0.123665	0.000144

Supplementary Information References

Burg, J.-P., Bodinier, J.-L., Gerya, T., Bedini, R.-M., Boudier, F., Dautria, J.-M., Prikhodko, V., Efimov, A., Pupier, E., Balanec, J.-L. (2009) Translithospheric Mantle Diapirism: Geological Evidence and Numerical Modelling of the Kondyor Zoned Ultramafic Complex (Russian Far-East). *Journal of Petrology* 50, 289-321.

Cabri, L.J., Stern, R.A., Czamanske, G.K. (1998) Osmium isotope measurements of the Pt-Fe alloy placer nuggets from the Konder Intrusion using a Shrimp II Ion Microprobe. *8th International Platinum Symposium Abstracts*, 55-58.

Chaika, I.F., Izokh, A.E. (2018) Dunites of the Inagli massif (Central Aldan), cumulates of lamproitic magma. *Russian Geology and Geophysics* 59, 1450-1460.

Coggon, J. A. Nowell, G.M., Pearson, D.G., Oberthuïr, T., Lorand, J.-P., Melcher, F., Parman, S.W. (2012) The 190Pt-186Os decay system applied to dating platinum-group element mineralization of the Bushveld Complex, South Africa. *Chemical Geology* 302-303, 48-60.

Day, J.M.D., Walker, R.J., Warren, J.M. (2017) ^{186}Os-^{187}Os and highly siderophile element abundance systematics of the mantle revealed by abyssal peridotites and Os-rich alloys. *Geochimica et Cosmochimica Acta* 200, 232-254.

Fonseca, R.O.C, Brückel, K., Bragagni, A., Leitzke, F.P., Speelmanns, I.M., Wainwirght, A.N. (2017). Fractionation of rhenium from osmium during noble metal alloy formation in association with sulfides: Implications for the interpretation of model ages in alloy-bearing magmatic rocks. *Geochimica et Cosmochimica Acta* 216, 184-200.

Kononova,V.A., Pervov,V.A., Bogatikov, O.A., Mus-Shumacher, U., Keller, I. (1995). Mesozoic potassic magmatism of the Central Aldan: Geodynamics and genesis. *Geotectonics* 29, 224-234.

Luguet, A., Nowell, G.M., Pearson, D.G. (2008). ^{184}Os/^{188}Os and ^{186}Os/^{188}Os measurements by negative thermal ionisation mass spectrometry (NTIMS): Effects of interfering element and mass fractionation corrections on data accuracy and precision. *Chemical Geology* 248, 342-362.

Malitch, K.N., Thalhammer, O.A.R. (2002) Pt–Fe nuggets derived from clinopyroxenite–dunite massifs, Russia: a structural, compositional and osmium-isotope study. *The Canadian Mineralogist* 40, 395-418.

Malitch, K.N., Efimov, A.A., Badanina, I.Yu. (2012) The Age of Kondyor Massif Dunites (Aldan Province, Russia): First U–Pb Isotopic Data. *Doklady Earth Sciences* 446, 1054-1058.

Nekrasov, I.Y., Lennikov, A.M., Zalishchak, B.L., Oktyabrsky, R.A., Ivanov, V.V., Sapin, V.I., Taskaev, V.I (2005) Composition variations in platinum-group minerals and gold, Konder alkaline-ultrabasic massif, Aldan Shield, Russia, *The Canadian Mineralogist* 43, 637-654.

Nowell, G.M., Luguet, A., Pearson, D.G., Horstwood, M.A. (2008a). Precise and accurate ^{186}Os/^{188}Os and ^{187}Os/^{188}Os measurements by Multi-Collector Plasma Ionisation Mass Spectrometry (MC-ICP-MS) part I: solution analyses. *Chemical Geology* 248, 363-393.

Nowell, G.M., Pearson, D.G., Parman, S.W., Luguet, A., and Hanski, E. (2008b) Precise and accurate ^{186}Os/^{188}Os and ^{187}Os/^{188}Os measurements by Multi-Collector Plasma Ionisation Mass Spectrometry, part II: The application of laser ablation MC-ICPMS to single-grain Pt-Os and Re-Os geochronology in platinum group alloy grains. *Chemical Geology* 248, 394-426.

Orlova, M. P. (1992). Geology and genesis of the Konder Massif. *Geology of the Pacific Ocean* 8, 120-132.

Pearson, D.G., Parman, S.W., Nowell, G.M. (2007) A link between large mantle melting events and continent growth seen in osmium isotopes. *Nature* 449, 202-205.

Pushkarev Yu.D., Kostoyanov, A.I., Orlova, M.P., Bogomolov, E.S. (2002): Peculiarities of the Rb-Sr, Sm-Nd, Re-Os and K-Ar isotope systems in the Kondyor massif: mantle substratum, enriched by PGE. *Regional geology and metallogeny* 16, 80-91 (in Russ.)

Savatenkov, V.M., Mochalov, A.G. (2018) Age and Sources of Dunite from the Konder Massif (Aldan Shield). *Doklady Earth Sciences* 482, 1331-1335

Shcheka, G.G., Lehmann, B., Gierth, E., Gömann, K., Wallianos, A. (2004) Macrocrystals of Pt–Fe alloy from the Kondyor PGE placer deposit, Khabarovskiy Kray, Russia: trace-element content, mineral inclusions and reaction assemblages. *The Canadian Mineralogist* 42, 601-617.

Shukolyukov, Yu.A., Yakubovich, O.V., Mochalov, A.G., Kotov, A.B., Sal'nikova, E.B., Yakovleva, S.Z., Korneev, S.I., Gorokhovskii, B.M. (2012) New Geochronometer for the Direct Isotopic Dating of Native Platinum Minerals (190Pt-4He Method). *Petrology* 20, 491-507.

Simonov, V.A., Prikhod'ko, V.S., Kovyazin, S.V., Tarnavsky, A.V. (2010) Crystallization Conditions of Dunites in the Konder Platiniferous Alkaline–Ultramafic Massif of the Southeastern Aldan Shield, *Russian Journal of Pacific Geology* 4, 429-440.

Tommasi, A., Vauchez, A., Ionov, D.A. (2008) Deformation, static recrystallization, and reactive melt transport in shallow subcontinental mantle xenoliths (Tok Cenozoic volcanic field, SE Siberia) *Earth and Planetary Science Letters* 272, 65–77.

Wainwright, A.N., Luguet, A., Schreiber, A., Fonseca, R.O.C., Nowell, G.M., Lorand, J.-P., Janney, P.E. (2016) Nanoscale variations in ^{187}Os isotopic compositions and HSE systematics in a Bultfontein peridotite. *Earth and Planetary Science Letters* 447, 61-70.